PNAS nexus

PNAS Nexus, 2022, **2**, 1–9
https://doi.org/10.1093/pnasnexus/pgac279
Advance access publication date: 12 December 2022
Research Report

Holographic realization of the prime number quantum potential

Donatella Cassettari [a,*], Giuseppe Mussardo [b] and Andrea Trombettoni [b,c]

[a]SUPA School of Physics and Astronomy, University of St. Andrews, North Haugh, St. Andrews KY16 9SS, UK
[b]SISSA and INFN, Sezione di Trieste, Via Bonomea 265, I-34136 Trieste, Italy
[c]Department of Physics, University of Trieste, Strada Costiera 11, I-34151 Trieste, Italy
*To whom correspondence should be addressed: Email: dc43@st-and.ac.uk
Edited By: J.C. Davis

Abstract

We report the experimental realization of the prime number quantum potential $V_N(x)$, defined as the potential entering the single-particle Schrödinger Hamiltonian with eigenvalues given by the first N prime numbers. Using computer-generated holography, we create light intensity profiles suitable to optically trap ultracold atoms in these potentials for different N values. As a further application, we also implement a potential whose spectrum is given by the lucky numbers, a sequence of integers generated by a different sieve than the familiar Eratosthenes's sieve used for the primes. Our results pave the way toward the realization of quantum potentials with arbitrary sequences of integers as energy levels and show, in perspective, the possibility to set up quantum systems for arithmetic manipulations or mathematical tests involving prime numbers.

Keywords: quantum devices, Schrödinger Hamiltonian, optical traps, prime numbers

Significance Statement:

Prime numbers are the building block of mathematics and their intriguing properties have been an endless subject of investigation and wonder. The approach pursued here is to regard them as energy levels of a quantum system. To this aim, we devise and experimentally implement the quantum potential of a Schrödinger Hamiltonian having the first N primes as eigenvalues. We also experimentally realize a quantum potential with a spectrum given by the first N lucky numbers, a sequence that can be considered as the "cousin" of the sequence of the primes. Being able to encode interesting sequences of integers in a quantum potential opens the possibility of addressing purely mathematical questions of number theory through quantum experiments.

Introduction

Mathematics is a gold mine of surprises, starting from its very basic branch: arithmetic. Consider as major examples the sets of the natural numbers

$$\mathbb{N} = \{1, 2, 3, 4, 5, \ldots\} \tag{1}$$

and of the prime numbers

$$\mathbb{P} = \{2, 3, 5, 7, 11, \ldots\}. \tag{2}$$

While the pattern of natural numbers is obvious, since no matter which one you pick, it is straightforward to determine what the next one is, the answer is instead highly nontrivial for the set of prime numbers, whose intriguing and sometimes apparently erratic properties never ceased to intrigue mathematicians, physicists, scientists, and curious people in general (1–9).

The sequences of natural and prime numbers are mathematical objects: one could say that they are the mathematical objects *par excellence*, being at the roots of arithmetic and therefore at the roots of entire mathematics. However, a useful point of view—particularly relevant for computational purposes—is to see them as quantities that emerge from physical operations performed in the physical world. The rationale is to have a physical system, an *abacus*, on which one performs the desired operations acting on the elements of certain sequences of integers. Since ultimately all aspects of the world around us can be explained using quantum mechanics, we would like to have a *quantum abacus*, i.e. a quantum system with energy levels related in a controllable way to sequences of integers.

Given the role played by prime numbers in many problems, from factorization of integers to celebrated conjectures of mathematics such as the Riemann hypothesis (10–12) or the Goldbach conjecture (13), it is desirable to find new ways in which prime numbers emerge from the experimental control of a quantum system. This is particularly important in view of several theoretical proposals to tackle problems from number theory using quantum mechanics ideas: prominent examples include Shor's algorithm (14), the factorization of large integers (15, 16), the computation of prime number functions by employing the so-called quantum prime state (17, 18), primality tests (19, 20), and attempts to

Competing Interest: The authors declare no competing interest.
Received: September 20, 2022. **Accepted:** December 7, 2022

establish the validity of the Riemann hypothesis [see refs. (21, 22) for reviews].

In this paper, with the aim of implementing a quantum abacus, we choose to consider discrete sequences of numbers as spectra of some quantum Hamiltonians. We focus on a particle of mass m in one dimension, with the Hamiltonian expressed in the standard form as

$$\hat{H} = \frac{p^2}{2m} + V(x), \tag{3}$$

where p is the momentum operator and $V(x)$ is taken to be a continuous function in a given interval $\mathcal{J}$ (which can be the entire real axis). If a potential $V_N(x)$ is such that the eigenvalues E_n of the time-independent Schrödinger equation

$$\hat{H}\psi_n = \left(-\frac{\hbar^2}{2m}\frac{d^2}{dx^2} + V_N(x)\right)\psi_n = E_n\psi_n \tag{4}$$

are the first N prime numbers, we call $V_N(x)$ a *prime number quantum potential*. In saying that the eigenvalues of Eq. 4 are the prime numbers, or any other sequence of integers, we are actually referring to the eigenvalues e_n of $\hat{H}$ defined in dimensionless units: in physical units, the eigenvalues E_n are equal to their dimensionless counterpart e_n multiplied by a constant having the dimension of an energy, which depends on $\hbar$, m, and a length characteristic of the potential $V_N(x)$ itself. To fix the notation, hereafter, the ground state in Eq. 4 corresponds to $n = 0$ (and therefore, in the case of the primes, $e_0 = 2$). For completeness, let us point out that in addition to the discrete part of the spectrum featuring the desired first N primes, the potential $V_N(x)$ will also have a continuous spectrum for energies larger than the highest prime p_N.

The experimental realization of $V_N(x)$ provides the first ingredient for the implementation of a kind of quantum abacus, in which arithmetic operations can be translated into physical operations on the quantum particle. As we will show, reproducing the desired sequence of eigenvalues is a challenging task because it requires control on the fine details of $V_N(x)$. Given the typical length scale of atom traps, one needs to control $V_N(x)$ at the scale of micrometers. In this regard, light sculpting techniques provide versatile tools to dynamically control and engineer optical potentials for neutral atoms. These techniques are based on devices such as spatial light modulators (SLMs), digital micromirror devices (DMDs), and scanning acousto-optic deflectors (AODs) (23). In particular, SLMs underpin computer-generated holography, in which a spatial phase modulation is applied to the trapping light such that a desired intensity distribution is realized in the far field. This leads to holographic optical traps, which have been employed in experiments ranging from single atoms to Bose–Einstein condensates (24). Therefore holographic techniques are a natural tool to implement the prime number quantum potential.

The aim of this paper is to present the experimental realization of such a potential. As discussed in detail in the next sections, the problem presents a number of interesting points, which touch on key theoretical and experimental questions in quantum mechanics with fascinating outputs in number theory. The paper is organized as follows: In the section "The intriguing prime numbers," we recall some basic features of the prime numbers, pointing out the main challenges one has to face to setup up a potential which has them as spectrum. In the section "Holographic techniques," we provide a brief insight into light sculpting techniques. In the section "Discrete sequences and quantum potentials," we present the theoretical framework of supersymmetric quantum mechanics (SQM) (25–27), which leads to the exact expression of $V_N(x)$, and we also discuss the pros and cons of this approach compared to a semiclassical determination of the prime number potential (19). In the section "Experimental prime number potentials," we present experimental prime number potentials suitable for atom trapping, and we assess the feasibility of a subsequent implementation with ultracold atoms. In the section "The lucky quantum potential," to further demonstrate the flexibility of our approach, we discuss the realization of another quantum potential associated to a different discrete sequence of integers, the so-called *lucky numbers*. This is an interesting set of integers, which may be regarded as "cousins" of the prime numbers, generated by a slightly different sieve than the familiar Eratosthenes's sieve which gives rise to the prime numbers (28). Finally, we draw our conclusions.

The intriguing prime numbers

A fundamental theorem of arithmetic states that every natural number >1 is either a prime number or a product of prime numbers. Hence, the prime numbers may be regarded as the atoms of arithmetic but, in contrast with the finitely many chemical elements, the number of primes is instead infinite, as shown by a classic argument by Euclid dated more than 2000 years ago. Besides this fundamental role in arithmetic, what makes the prime numbers intriguing is their bipolar personality, i.e. in the realm of mathematics, they are the perfect Dr Jekyll and Mr Hyde. Such an erratic behavior, almost an "insanity," emerges by looking at the short and large distance scales of these numbers. Indeed, at short scale, their appearance along the sequence of the integers is completely unpredictable but, on a large scale, their coarse graining properties, and in particular how many prime numbers there are below any real number x, are aspects that can be controlled with great precision. In other words, while there is no known simple function $f(n)$ that gives the nth prime number p_n [and the actual determination of prime numbers can only be done by means of the familiar Eratosthenes's sieve (5–9)], thanks to the insights of many prominent mathematicians (in particular Riemann), we have instead perfect knowledge of the inverse function $\pi(x)$, which counts the number of primes below the real number x (1–11, 29–32). Such a function has a staircase behavior (since it jumps by 1 each time x crosses a prime) but becomes smoother and smoother for increasing values of x. Its first estimate was empirically obtained by Gauss and Legendre as

$$\pi(x) \sim \frac{x}{\ln x}, \tag{5}$$

and, even though this formula may be considered just a coarse approximation of $\pi(x)$, it is nevertheless able to capture the asymptotic behavior of $\pi(x)$—a result that constitutes the content of the "Prime Number Theorem" (29–32):

$$\lim_{x\to\infty} \frac{\pi(x)\ln x}{x} = 1. \tag{6}$$

A more precise version of this estimate is given by $\pi(x) \simeq \mathrm{li}(x) \equiv \int_2^x \frac{dt}{\ln t}$, while a further refinement was provided by Riemann (10, 11) in terms of the series

$$\pi(x) \simeq R(x) = \sum_{m=0}^{\infty} \frac{\mu(m)}{m}\,\mathrm{li}\left(x^{1/m}\right), \tag{7}$$

with the Moebius numbers $\mu(m)$ defined by

$$\mu(m) = \begin{cases} 1 & \text{if } m = 1 \\ 0 & \text{if } m \text{ is divisible by a square of a prime} \\ (-1)^k & \text{otherwise} \end{cases}$$

where k is the number of prime divisors of the integer m. It is worth stressing that $R(x)$ is the smooth function that approximates $\pi(x)$ more efficiently and it is well known that to reproduce the actual staircase jumps of $\pi(x)$ one needs to employ the zeros of the Riemann zeta-function (7, 10, 11).

Knowing $\pi(x)$ helps us estimate the growth behavior of the nth prime number. Indeed, by setting $p_n = \pi^{-1}(n)$ and inverting at the lowest order the function $\pi(x)$ (for instance, using Gauss formula of Eq. 5), we have the following scaling law for the nth prime number:

$$p_n \simeq n \log n. \tag{8}$$

However, the true unpredictable nature of the primes becomes particularly evident if we focus our attention on their gaps: for every prime p_n, let $g(p_n)$ be the number of composite numbers between p_n and the next prime p_{n+1}, so that

$$p_{n+1} = p_n + g(p_n) + 1. \tag{9}$$

With this definition, $g(p_n)$ is the size of the gap between p_n and p_{n+1}. Using the scaling law of Eq. 8, we expect the average gap $\bar{g}(p_n)$ between p_n and p_{n+1} to go as $\bar{g}(p_n) \sim \log n$, but the interesting question is: how wide is the range of values of these gaps? There is an extensive literature on this topic, see, for instance, refs. (33–38), and hereafter we only underline some basic features that are important for our subsequent considerations.

The minimum value of $g(p)$ is 1 and is obtained for the twin primes, i.e. the pairs such as (17, 19) or (29, 31), etc., which differ by 2. Presently, it is not known whether or not there are infinitely many twin primes, although there are strong reasons to believe that the number of twin primes is indeed infinite [see, for instance, the heuristic arguments presented in ref. (6)]. On the other hand, it is quite easy to show that $g(p_n)$ can be arbitrarily large, so that

$$\lim_{n\to\infty} \sup g(p_n) = \infty. \tag{10}$$

To prove this result, consider an arbitrary integer $N > 1$ and the associated sequence of integers

$$N! + 2, N! + 3, N! + 4, N! + 5, ..., N! + N.$$

These $(N - 1)$ consecutive numbers are all composite and therefore, if p is the largest prime less than $N! + 2$, we have $g(p) > N - 1$. Since we can send $N \to \infty$, we arrive to the result of Eq. 10. In summary, the sequence of primes shows a pattern of the gaps which is not at all regular, for instance, one does not have any clue where the smallest gaps may appear.

These features highlight the irregular behavior of the primes and lead to the conclusion that the quantum potential $V_N(x)$ that encodes them should be a rather peculiar function. Given that it has N bound states with energies equal to the prime numbers and strong variations in the energy gap between consecutive levels, we expect $V_N(x)$ to display a rich structure of maxima and minima which depends on N. Hence, the experimental technique to realize $V_N(x)$ must be sufficiently flexible in order to accurately reproduce this structure. As shown in the next section, experimental techniques such as computer-generated holography start with sampling $V_N(x)$ over a number of points ("pixels"). With more pixels available, it is possible to increase the complexity of $V_N(x)$, hence the number of energy levels.

Holographic techniques

Before discussing how to obtain the exact expression of $V_N(x)$, let us review the experimental techniques that enable the optical realization of the prime number potentials. Our optical potentials are suitable for trapping ultracold atoms in a one-dimensional geometry via the optical dipole force. The optical dipole potential is proportional to the intensity of the light (39); hence, here we shape the intensity profile of an incoming laser beam using holographic techniques. In computer-generated holography, a liquid-crystal SLM spatially modulates the phase of the light. The phase pattern on the SLM acts as a generalized diffraction grating, so that in the far field, we have Fraunhofer diffraction and an intensity pattern is formed, which can be used to implement $V_N(x)$. The SLM acts effectively as a computer-generated hologram, and the light field in the output plane is the Fourier transform of the light field in the SLM plane. The calculation of the appropriate phase modulation to give the required output field is a well-known inverse problem that, in general, requires numerical solutions. Here, we use a conjugate gradient minimization technique which efficiently minimizes a specified cost function (40, 41). The cost function is defined to reflect the requirements of the chosen light field in the output plane. In addition to specifying the intensity profile of the field, which gives $V_N(x)$, we also constrain the phase of the light in the output plane. Namely, a uniform phase is programmed across the whole intensity profile. Controlling the phase this way leads to a well-maintained intensity profile as the light propagates out of the output plane.

Figure 1 is a schematic of the experimental setup. Our SLM (Hamamatsu LCOS-SLM X10468) is illuminated by laser light with wavelength 1064 nm. The light diffracted by the SLM is focussed on the output plane by a $f = 75$ mm achromatic doublet (Thorlabs AC508-075-B), and detected by a CCD camera (Thorlabs DCU224M). As shown in the figure, in order to accurately reproduce a given target light profile, we program only a small subset of the output plane [the "signal region" (SR)], whereas the field is left unconstrained in the rest of the plane (42). We use the following cost function (41):

$$C = 10^d \left(1 - \sum_{p,q\in \mathrm{SR}} \mathrm{Re}\left\{\left|\tilde{\tau}^*_{p,q}\tilde{E}^{\mathrm{out}}_{p,q}\right|\right\}\right)^2, \tag{11}$$

where p and q denote the output plane coordinates. Here, $\tau_{p,q}$ is the target light field, $E^{\mathrm{out}}_{p,q}$ is the output light field, linked to the SLM light field via a Fourier transform, and the over-tilde denotes normalization over the SR. This cost function minimizes the discrepancy between $\tau_{p,q}$ and $E^{\mathrm{out}}_{p,q}$ in the parameter space of all the different phase distributions that the SLM can generate. The prefactor 10^d, where $d = 9$ for the results shown here, increases the steepness of the cost function to improve convergence time and accuracy.

In the algorithm, both the SLM plane and the output plane have a size of $2m \times 2m$ pixels, where $m \times m$ is the number of pixels in the SLM array: namely, the SLM plane is "padded" with zeroes to increase its size from $m \times m$ to $2m \times 2m$. The purpose of this is to fully resolve the output plane (42). We find that with 512×512 SLM pixels available, we achieve 1D potentials that are up to 100-pixel long in the output plane. This amounts to about 1/10 of the linear dimension of the 1024×1024 output plane. If we increase the length of the potential beyond this, we lose light-utilization

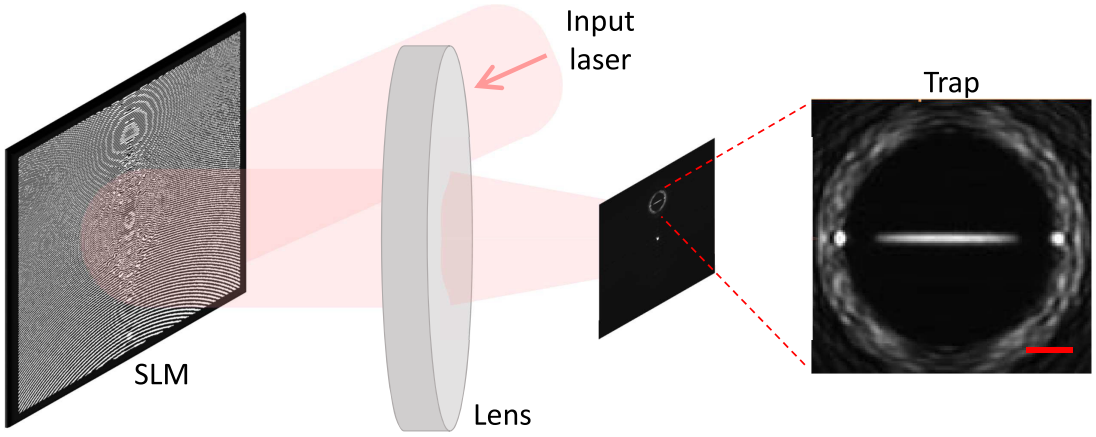

Fig. 1. Experimental setup, showing the phase profile imprinted by the SLM and the resulting light intensity profile in the trapping plane. The zoomed-in image shows the SR, i.e. the region of the output plane in which the field is programmed by the conjugate gradient minimization algorithm. In this case, the SR contains a generic 1D trapping potential. The circular intensity distribution delimitates the boundary with the region of the output plane where the intensity is left unconstrained. The scale bar is 100 μm.

efficiency, i.e. the light intensity in the pattern becomes too low. With our holographic method, we can obtain any smoothly varying intensity profile over this 100-pixel interval. However, given the nontrivial behavior of the potential described at the end of the previous section, this 100-pixel maximum interval limits the number of energy levels of the potential, i.e. the number of primes. Therefore, we envisage that to increase the number of primes contained in the potential beyond what we present in this work, it is necessary to increase the number of SLM pixels.

In future, it will be possible to realize prime number potentials also with light sculpting techniques which are alternative to the liquid-crystal SLM we use in this work. For instance, AODs have been used to realize a wide range of optical potentials (43, 44). While the AOD potentials realized so far are simpler than the prime number potentials presented here, it is possible in principle to increase their level of complexity. Another possibility is the use of DMDs. A DMD is a matrix of individually addressable mirrors which can be used as an intensity mask that can be directly imaged on the atoms. The projected image from a DMD is intrinsically binary, due to the individual mirrors being either "on" or "off"; however, there are methods that overcome this limitation and allow the realization of intensity gradients: half-toning and time-averaging (23). Half-toning relies on the finite optical resolution of the imaging optical system, whereby multiple mirrors contribute to each resolution spot in the projected plane. This provides a number of possible intensity levels in each resolution spot, which is given by the number of contributing mirrors. In (45), half-toning was used to demonstrate 1D potentials with a high degree of control. If half-toning is combined with time-averaging, in which a time-averaged potential is achieved with high-speed modulation of the mirrors, intensity control can be further improved. With this combination of approaches, it will be possible to use DMDs to reproduce the prime number potentials presented here. The DMD dimension required for this is comparable to the dimension of the liquid-crystal SLM we use here, making the two techniques equivalent.

Discrete sequences and quantum potentials

Let us now address the problem of how to design, in general, a quantum potential $V(x)$ in such a way that a given sequence of real numbers

$$\mathcal{E} = \{e_0, e_1, e_2, e_3, \ldots\} \tag{12}$$

coincides with the set of eigenvalues of the Schrödinger equation shown in Eq. 4. It is important to distinguish two cases:

- The sequence $\mathcal{E}$ is *infinite*. In this case, a necessary condition for the existence of a continuous potential $V(x)$ able to support the sequence $\mathcal{E}$ as spectrum is that asymptotically the e_n's satisfy the bound (19)

$$e_n \leq A\, n^2, \quad n \to \infty, \tag{13}$$

  where A is a positive real number.
- The sequence $\mathcal{E}$ is, on the contrary, *finite*, i.e. it only consists of a finite number N of terms, $e_0, e_1, e_2, \ldots, e_{N-1}$, plus possibly a continuous part of the spectrum with energies larger than the maximum value of the e_n's. In this case, there is no obstacle to the existence of a potential $V(x)$ which supports such a spectrum, and the explicit form of this potential can indeed be found using methods of SQM (25), as discussed below.

A familiar example of the first case is provided by the infinite set $\mathbb{N}$ of all natural numbers, whose corresponding potential $V(x) \propto x^2$ gives rise to the well-known Hamiltonian of the harmonic oscillator (46). Another example is provided by the sequence $\mathcal{E} = \{1, 4, 9, 16, \ldots\}$ of squared integers, which can be realized as a quantum spectrum in terms of a properly tuned infinite-well potential (46). It is important to underline that, besides these known cases and very few others, it is in general *not* known a universal procedure for engineering a potential $V(x)$ with *exactly* all elements of an infinite sequence $\mathcal{E} = \{e_0, e_1, e_2, e_3, \ldots\}$ as eigenvalues. The best one can do in such a case is to identify a *semiclassical* potential $V_{sc}(x)$: it is worth to stress, however, that this quantity is only able to capture the scaling growth of the eigenvalues rather their actual values, since it is determined by the formula

$$x(V_{sc}) = \frac{\hbar}{\sqrt{2m}} \int_{E_0}^{V_{sc}} \frac{dE}{\frac{dE}{dn}\sqrt{V_{sc} - E}}, \tag{14}$$

which depends upon the density of states dE/dn rather than the individual energy levels e_n's. Taking, for instance, the infinite set $\mathbb{P}$ of the primes, it is easy to see that these numbers satisfy the bound (13) (see Eq. 8). The corresponding semiclassical potential

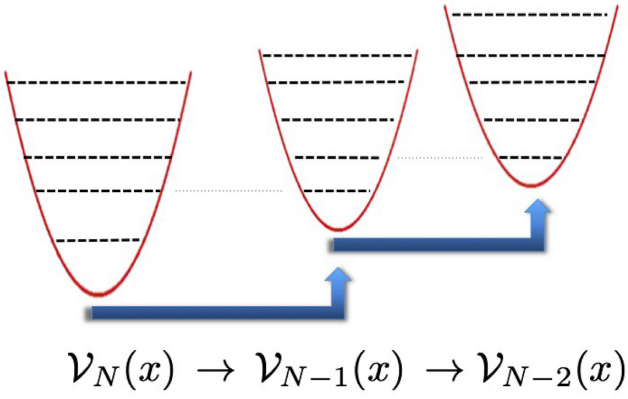

Fig. 2. Sequence of supersymmetric partner potentials $\mathcal{V}_k(x)$, where $\mathcal{V}_k$ shares all the spectrum of the previous one $\mathcal{V}_{k+1}$ except its ground state energy.

was determined in (19) by substituting in Eq. 14 the density of states coming from Eq. 7:

$$\left(\frac{dE}{dn}\right)^{-1} = \frac{d\pi}{dE} \simeq \frac{1}{\log E}\sum_{m=1}^{\infty}\frac{\mu(m)}{m}E^{(1-m)/m}. \tag{15}$$

Let us now consider the second case, where the sequence $\mathcal{E} = \{e_0, e_1, e_2, e_3, \ldots\}$ is instead finite. Here, there exists the general procedure of SQM (25) for engineering a potential $\mathcal{V}(x)$ with the e_n's as its *exact* spectrum. It is well known that there are many potentials that share the same spectrum (47), and to identify uniquely one of these potentials, in the following we impose the additional condition $\mathcal{V}(x) = \mathcal{V}(-x)$. Using the methods of SQM, one sets up a chain of potentials $\mathcal{V}_k(x)$ ($k = N, N-1, \ldots, 0$), as those shown in Fig. 2, with the property that the potential $\mathcal{V}_{k-1}(x)$ has the *same* spectrum as the previous one $\mathcal{V}_k(x)$, *except* its ground state. In other words, climbing down in the label k of these potentials $\mathcal{V}_k(x)$, there is a depletion, one by one, of the lowest level of the previous potential. This chain of potentials is determined by a system of differential equations and, as we shall see below, this structure is at the root of the exact reconstruction of the potential with a given set of energy levels. Indeed, it is sufficient to reverse the procedure and adjust, one by one, all the desired eigenvalues! With a finite set of discrete eigenvalues, the final potential has a finite limit at $x \rightarrow \pm\infty$ and therefore also has a continuum part of the spectrum; however, this is not relevant for our purposes and will not be discussed further. In more detail, the top-down procedure works as follows (25):

(1) First of all, we subtract from all the eigenvalues e_n the highest one e_N, so that the new set of numbers $\{\tilde{E}_n\}$

$$\tilde{E}_k = e_{N-k} - e_N \quad , \quad k = 0, 1, \ldots, N, \tag{16}$$

will be considered as the new spectrum. The $\tilde{E}_k$'s are of course the (negative) gaps computed from the *highest* eigenvalue e_N. Notice that, consistently, they are enumerated starting from the top to the bottom, so $\tilde{E}_0 = 0$, $\tilde{E}_1$ is the first gap, $\tilde{E}_2$ the second gap, and so on. A potential $\mathcal{V}(x)$ where its only eigenvalue is $\tilde{E}_0 = 0$ is of course $\mathcal{V}_0(x) = 0$. This potential is used as input for the Riccati equation for the superpotential $W_1(x)$

$$W_1'(x) - W_1^2(x) + \mathcal{V}_0(x) = \tilde{E}_1 \tag{17}$$

with boundary condition $W_1(0) = 0$.

(2) Once such a function $W_1(x)$ has been obtained, one can construct another potential $\mathcal{V}_1(x)$ as

$$\mathcal{V}_1(x) = 2\tilde{E}_1 + 2W_1^2(x) - \mathcal{V}_0(x). \tag{18}$$

This potential is then substituted into Eq. 17 (i.e. $\mathcal{V}_0(x) \rightarrow \mathcal{V}_1(x)$, substituting also $\tilde{E}_1 \rightarrow \tilde{E}_2$), so that one has a differential equation for another super-potential $W_2(x)$

$$W_2'(x) - W_2^2(x) + \mathcal{V}_1(x) = \tilde{E}_2. \tag{19}$$

(3) Proceeding iteratively in this way, one has a recursive sequence of differential equations

$$W_k'(x) - W_k^2(x) + \mathcal{V}_{k-1}(x) = \tilde{E}_k,$$

$$\mathcal{V}_k(x) = 2\tilde{E}_k + 2W_k^2(x) - \mathcal{V}_{k-1}(x), \tag{20}$$

all of them solved with the boundary condition $W_k(0) = 0$, which ensures that the final potential $\mathcal{V}(x) = \mathcal{V}_N(x)$ is an even function. This recursive system is continued until all the gaps have been taken into account. Hence, solving (in general numerically) the differential equations of Eq. 20, one arrives to the Hamiltonian which has *exactly* the spectrum $\{e_n\}$

$$H = -\frac{d^2}{dx^2} + \mathcal{V}_N(x) + e_N. \tag{21}$$

These are indeed the theoretical steps which lead to the potential $V_N(x)$ with *exactly* the first N prime numbers (26, 27), in other words, our quantum abacus with a finite number of beads. From what is discussed above, the pros and cons of the SQM method are fairly evident:

- *Pros*: The method is *exact*, i.e., given a finite set of numbers $\{e_n\}$, this method provides the *exact* potential which has these numbers as the exact eigenvalues. If this set is made of the first N primes, the potential exactly accommodates these prime numbers in the spectrum.
- *Cons*: The method is *not* smoothly scalable, in the sense that if we have determined the potential which has as eigenvalues a set of N values e_n, when adding a new value e_{N+1}, we have to start again from scratch and determine altogether another potential that will accommodate *exactly* the $(N+1)$ eigenvalues.

In comparison, the semiclassical potential $V_{sc}(x)$ (e.g. for the primes) has somehow opposite pros and cons: it is scalable, in the sense that once it has been implemented, all its eigenvalues are fixed but, on the other hand, it is not exact, i.e. its eigenvalues are not exactly the prime numbers.

In closing this section, it is important to stress two important mathematical properties of the system of differential equations shown in Eq. 20. The first property is that there is one and *only one* family of potentials which provide closed analytical solutions of the system of differential equations and which recursively reproduce themselves at each step of the procedure. This is the family of the Pöschl–Teller potentials given by

$$\hat{V}_N(x) = -\frac{1}{2}\frac{N(N+1)}{\cosh^2 x}, \tag{22}$$

associated with the exact sequence of gaps

$$\tilde{E}_n = -\frac{n^2}{2}, \quad n = 0, 1, 2, \ldots N. \tag{23}$$

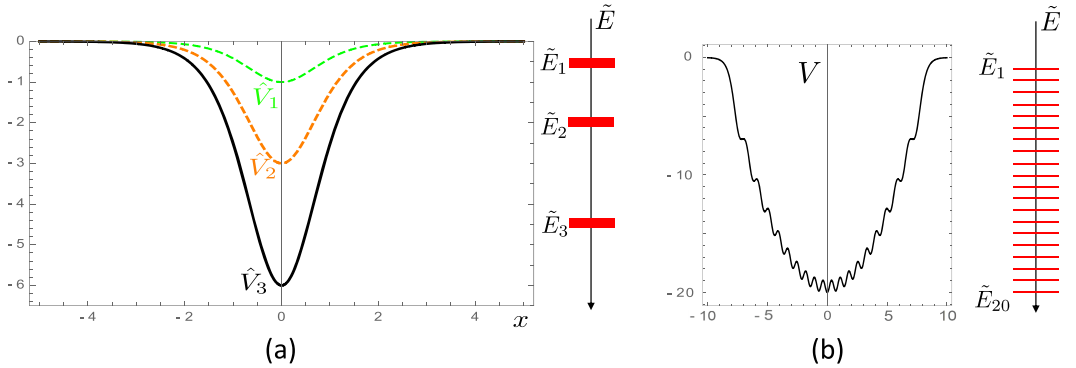

Fig. 3. (a) Sequence of Pöschl–Teller potential $\hat{V}_N(x)$ obtained by solving the recursive differential Eqs. 20 to accommodate the energy gaps shown on the right hand side. (b) Potential $V(x)$ which has exactly the first (negative) 20 natural numbers as energy gaps.

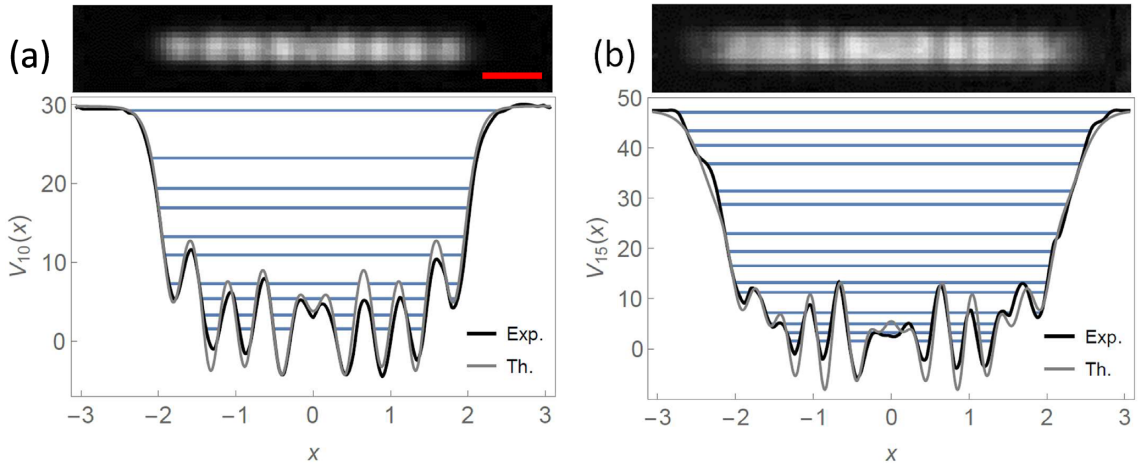

(c)

Prime numbers	2	3	5	7	11	13	17	19	23	29	31	37	41	43	47
e_n for $V_{10}(x)$	1.58	3.31	5.40	7.33	10.9	13.2	16.9	19.4	23.2	29.3					
e_n for $V_{15}(x)$	1.58	3.21	5.00	7.22	11.3	13.2	16.6	19.4	22.9	28.8	31.4	36.9	40.6	43.4	47.1

Fig. 4. (a and b) Experimental prime number potentials $V_{10}(x)$ and $V_{15}(x)$. The images show the light intensity profiles, where the red scale bar is 50 μm, applicable to both images. The plots show the corresponding potentials, rescaled to dimensionless units, alongside their theoretical counterparts. The experimental eigenvalues are shown as horizontal lines on the plots and are also tabulated in (c), alongside the first 15 prime numbers for comparison.

The Pöschl–Teller potentials $\hat{V}_N(x)$ do not have oscillations and present the typical shape of an inverted bell (see Fig. 3a). The second property is that any finite sequence $\tilde{E}$ of gaps *other* than the one given by Eq. 23 is expected to give rise to a potential with *oscillations*. This is true even for very straightforward sequences, as, for instance, the potential which has exactly the sequence of the first 20 negative integers as its energy gaps, see Fig. 3b. This feature is also pretty evident in our realizations of the prime potentials: in Fig. 4, we show, for instance, the potentials $V_{10}(x)$ and $V_{15}(x)$, which have, as eigenvalues, exactly the first 10 and 15 prime numbers, respectively. These potentials have a number of oscillations which scales with the number of eigenvalues. These oscillations are expected to be more pronounced in correspondence to more irregular sequences of numbers chosen to be eigenvalues. This is certainly the case for the prime numbers, as underlined earlier.

Experimental prime number potentials

We use the apparatus shown in Fig. 1 to realize the prime number potentials $V_{10}(x)$ and $V_{15}(x)$. The experimental light intensity profiles and the corresponding potentials are shown in Fig. 4a and b. The potentials are meant to be implemented with light that is red-detuned relative to the atomic transition, so that regions of higher intensity correspond to a lower value of the potential (39). The potentials are rescaled so that they are plotted in dimensionless units alongside their theoretical counterparts. [See code and data available online (48).] The conversion between dimensionless eigenvalues e_n and physical eigenvalues E_n is given by

$$\frac{E_n}{e_n} = \frac{\hbar^2}{m}\left(\frac{l}{L}\right)^2, \tag{24}$$

where l and L are the lengths of the potential in dimensionless and physical units, respectively. Assuming ^{87}Rb atoms, we obtain $E_n/e_n = h \times 0.029\,\text{Hz}$ for $V_{10}(x)$ and $E_n/e_n = h \times 0.026\,\text{Hz}$ for $V_{15}(x)$. The potential depth can be calculated with the same conversion formula, leading to a depth of $k_B \times 47\,\text{pK}$ for $V_{10}(x)$ and of $k_B \times 69\,\text{pK}$ for $V_{15}(x)$. These figures show that we have shallow traps with very low trap frequencies, and that we would need to work at extremely cold temperatures, beyond what has been experimentally realized (49, 50).

However trap depths and trap frequencies can be increased by increasing the numerical aperture of the optical system, i.e. with

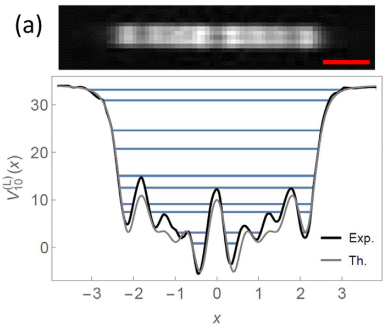

(b)

Lucky numbers	e_n for $V_{10}^{(L)}(x)$
1	0.85
3	3.16
7	7.45
9	9.12
13	12.6
15	15.1
21	20.7
25	24.6
31	30.9
33	33.2

Fig. 5. (a) Experimental lucky number potential $V_{10}^{(L)}(x)$, where the red scale bar is 50 μm. The corresponding eigenvalues are tabulated in (b) alongside the first 15 lucky numbers.

stronger focusing in conjunction with a larger SLM physical size. Our current optical system has a resolution spot of 10 μm. This determines the typical distance between peaks in the potentials, which is about three times the resolution spot. If in the future we use a resolution of 1 μm, e.g. with a quantum gas microscope (51, 52), then the distance between peaks and the overall physical length of the potentials can be scaled down accordingly. As shown in Eq. 24, energies scale with the inverse square of the physical length L. Hence, it will be possible to achieve trap depths of several nK, therefore improving experimental feasibility. In general, the length–depth aspect ratio of the potential is constrained: to increase the energy scale and correspondingly the potential depth, while at the same time maintaining the same number of energy levels and their relative spacing, it is necessary to scale down the physical length of the potential.

The experimental eigenvalues, expressed in dimensionless units, approximate the primes well. The potentials reported in Fig. 4 are stable in time, but sensitively depend on the alignment of the optical setup. Out of many experimental implementations we have obtained, the figure shows the optimized potentials, i.e. those whose eigenvalues match the primes if rounded to the nearest integer, as shown in Fig. 4c. The residual differences between the experimental eigenvalues and the primes arise from the discrepancies between the theoretical and experimental potentials, small but visible in the plots, which in turn are caused by an imperfect SLM response and by aberrations in the optical setup. The root-mean-square (r.m.s.) fractional discrepancy between the theoretical and the experimental potentials is 10% for $V_{10}(x)$ and 7% for $V_{15}(x)$, giving an r.m.s. fractional discrepancy between the eigenvalues and the primes of 8% and 6%, respectively. In future, these errors can be reduced with error-correction algorithms as shown in ref. (23). Another source of experimental uncertainty is due to the optical power on the SLM fluctuating over time, as this will change the eigenvalues. Specifically, a 1% fluctuation in the optical power leads to a $\sim 0.5\%$ change in the relative position of the eigenvalues. Hence, to achieve the three-digit precision shown in Fig. 4c, it is necessary to stabilize the optical power to 1%, which is feasible with active stabilization techniques.

The lucky quantum potential

The method presented in this paper can be straightforwardly extended to other sequences of integers. As a significant example related to the primes, we present here the potential $V_N^{(L)}(x)$ having as eigenvalues the so-called lucky numbers

$$\mathbb{L} = \{1, 3, 7, 9, 13, 15, 21, 35, 31, 33, \ldots\}. \tag{25}$$

These numbers, introduced in the 50s by Gardiner, Lazarus, Metropolis, and Ulam (28), are obtained with a sieve (known as the sieve of Josephus Flavius) different from the sieve of Eratosthenes used for the primes. Briefly, to obtain the prime numbers, one famously eliminates from the list of integers the multiples of 2 (the even numbers), then the multiples of 3, then the multiples of 5, and so on. On the contrary, for the lucky numbers, one eliminates numbers based on their position in the remaining set, instead of their original value, i.e. their position in the initial set of natural numbers. So, one eliminates every second number (again the even numbers), then, rescaling the remaining set, every third number (since the first number remaining in the list after 1 is 3), then every seventh number (since the first number remaining in the list after 3 is 7), and so on. As for the primes, there are infinitely many lucky numbers. Moreover, the prime numbers and the lucky numbers share many properties, including the asymptotic behavior according to the prime number theorem. A "lucky prime" is a lucky number that is also a prime, and it has been conjectured that there are infinitely many lucky primes.

Proceeding as in the earlier sections, in Fig. 5 we present, as an example, the experimental realization of the potential $V_{10}^{(L)}(x)$ for the first 10 lucky numbers. Notice that, using the transmission and reflection properties of a quantum potential, it is possible to set up a simple physical experiment, shown in Fig. 6, to test whether a given number $\mathbf{w}$ is both a lucky and a prime number. It involves a generalization of the proposal originally made in ref. (19) for checking the primality of a number: in the present case, let us imagine that in the box A we have realized the lucky potential $V_M^{(L)}$ with a number of levels M large enough so that $L_M \gg \mathbf{w}$, while in the box B, we have instead realized the prime number potential $V_N(x)$ with $p_N \gg \mathbf{w}$. Both potentials can be rounded and truncated at an energy cutoff ϵ_0 (which can be controlled by an external handle) in such a way that the original energy levels are essentially left unperturbed, but there are now asymptotic free states. Hence, we can take advantage of the typical resonance phenomena of quantum mechanics. We send on the composite apparatus G, made of A and B, a wave-packet from the left ($x \to -\infty$) with dimensionless energy $\mathbf{w}$. If the number $\mathbf{w}$ is a lucky number, it will be completely transmitted through box A, and if it is also a prime number, it will be completely transmitted through box B as well. Therefore, if the particle with energy $\mathbf{w}$ is observed coming out the apparatus G, then the number $\mathbf{w}$ is both a lucky and a prime number. This way, one could implement an experimental setup to test whether or not any given number $\mathbf{w}$ is a lucky prime.

Conclusions

In this paper, we have provided the first experimental realization of the prime number quantum potential $V_N(x)$, whose single-particle quantum Hamiltonian has the lowest N prime numbers as eigenvalues. The exact theoretical shape of this potential has been determined using SQM, and experimentally implemented by means of holographic techniques. As a proof of principle, we have experimentally realized the potential $V_N(x)$ with $N = 10$ and $N = 15$, finding a good agreement of the eigenvalues of these potentials with the first 15 prime numbers. We have also discussed how this procedure can be successfully used to implement potentials having other sequences of integer or real numbers as eigenvalues. As an example, in this paper we discussed the "lucky" potential $V_N^{(L)}(x)$, i.e. the potential that has the first N lucky numbers as eigenvalues, and we experimentally realized the case $N = 10$. Work is in progress to realize quantum potentials which have as energy spectra sequences such as the Fibonacci numbers (53),

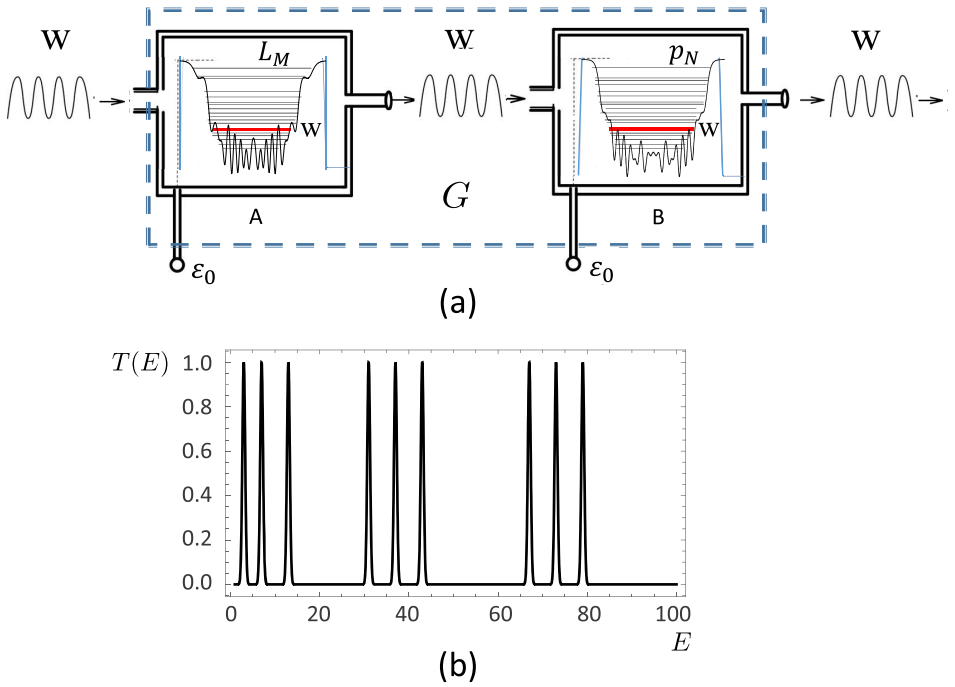

Fig. 6. (a) The G-apparatus filter numbers that are both lucky and prime numbers. The devices A and B are made of the potentials $V_M^{(L)}(x)$ and $V_N(x)$ for the M lucky numbers and N prime numbers, respectively, with an energy cutoff ϵ_0. (b) The transmission amplitude $T(E)$ versus the (dimensionless) energy E from the G-apparatus, with sharp resonance peaks in correspondence of those values of E that are both lucky and prime numbers.

or the real sequence of the logarithms of the integers, or of the logarithms of the primes, as considered in (15, 16, 54). Indeed, as we have already emphasized, any finite sequence of integer or real numbers can be obtained. One can also construct higher-dimensional potentials starting from the 1D potentials presented here. Another interesting future development is the use of the prime number potential and its eigenfunctions to study the entanglement entropy of a truncated version of the prime state introduced in (17, 18).

It goes without saying that, in order to increase the capability of the present device so as to have longer sequences as energy levels, of course one needs to increase its resolution, as is the case for any physical system which stores and manipulates numbers. In particular, for us this means increasing the number of SLM pixels used to sample the potential.

The present results provide a physical setup for a quantum mechanical manipulations of discrete sequences of numbers. This paves the way toward using these potentials for a variety of mathematical tests (such as the primality test) and arithmetic manipulations (such as prime factorization) by means of quantum experiments. It will be interesting to populate the energy levels with neutral atoms (bosonic or fermionic) and to induce transitions between levels by "shaking" the potential, either in terms of varying its overall strength or its center of mass, using a periodic drive. A compelling aspect is to determine whether it is better to employ for such manipulations either fermionic or bosonic atoms. Preliminary results seem to favor the latter, in absence of sizable atomic interactions, and further work is currently in progress. Equally interesting is to address other important open problems related to temperature effects and to the role played by atomic interactions, which can be controlled with Feshbach resonances (55), in view of the efficient implementation of arithmetic operations on integers.

Acknowledgments

We would like to thank G. D. Bruce for technical assistance.

Authors' Contributions

D.C. contributed to the experimental part of the work, while G.M. and A.T. contributed to its theoretical part.

References

1. Hardy GH, Wright EM. 1979. An introduction to theory of numbers. Oxford: Oxford University Press.
2. Apostol TM. 1998. Introduction to analytic number theory. 5thed. New York (NY): Springer.
3. Tao T. 2011. Structure and randomness in the prime numbers. In: Schleicher D, Lackmann M, editors. An invitation to mathematics. Berlin, Heidelberg: Springer.
4. Ore O. 1948. Number theory and its history. New York (NY): McGraw–Hill.
5. Ribenboim P. 1996. The new book of prime number records. Berlin: Springer-Verlag.
6. Schroeder MR. 1990. Number theory in science and communication. Berlin: Springer-Verlag.
7. Zagier D. 1977. The first 50 million prime numbers. Math Intell. 1:7–19.
8. Granville A, Martin G. 2006. Prime number races. Am Math Month. 113(1):1–33.
9. Rose HE. 1994. A course in number theory. Oxford: Oxford Science Publications.
10. Riemann GFB. 1859. Über die Anzahl der primzahlen unter einer gegebenen Grösse. Berlin: Monatsberichte der Königlichen Preussische Akademie des Wissenschaften. p. 671–680.

11. Edwards HM. 1974. Riemann zeta function. New York (NY): Academic Press.
12. Borwein P, Choi S, Rooney B, Weirathmueller A. 2007. The Riemann hypothesis: a resource for the afficionado and virtuoso alike. New York: Springer.
13. Rassias MT. 2017. Goldbach's problem: selected Topics. Cham: Springer International Publishing.
14. Shor PW. 1997. Polynomial-time algorithms for prime factorization and discrete logarithms on a quantum computer. SIAM J Comput. 26:1484.
15. Weiss C, Page S, Holthaus M. 2004. Factorising numbers with a Bose–Einstein condensate. Physica A. 341:586–606.
16. Gleisberg F, Di Pumpo F, Wolff G, Schleich WP. 2018. Prime factorization of arbitrary integers with a logarithmic energy spectrum. J Phys B At Mol Opt Phys. 51:035009.
17. Latorre JI, Sierra G. 2014. Quantum computation of prime number functions. Quantum Inf Comput. 14:577–588.
18. Latorre JI, Sierra G. 2015. There is entanglement in the primes. Quantum Inf Comput. 15:622–659.
19. Mussardo G. 1997. The quantum mechanical potential for the prime numbers. arXiv:cond-mat/9712010. https://doi.org/10.48550/arXiv.cond-mat/9712010, preprint: not peer reviewed.
20. Donis-Vela A, Garcia-Escartin JC. 2017. A quantum primality test with order finding. Quantum Inf Comput. 17:1143–1151.
21. Schumayer D, Hutchinson DAW. 2011. *Colloquium*: physics of the Riemann hypothesis. Rev Mod Phys. 83:307.
22. Wolf M. 2020. Will a physicist prove the Riemann hypothesis? Rep Prog Phys. 83:036001.
23. Gauthier G, *et al.* 2021. Dynamic high-resolution optical trapping of ultracold atoms. Adv Atomic Mol Opt Phys. 70:1–101.
24. Amico L, *et al.* 2021. Roadmap on atomtronics: state of the art and perspective. AVS Quantum Sci. 3:039201.
25. Cooper F, Khare A, Sukhatme U. 1995. Supersymmetry and quantum mechanics. Phys Rep. 251:267–385.
26. Ramani A, Grammaticos B, Caurier E. 1995. Fractal potentials from energy levels. Phys Rev E. 51:6323.
27. van Zyl BP, Hutchinson DA. 2003. Riemann zeros, prime numbers, and fractal potentials. Phys Rev E. 67:066211.
28. Gardiner V, Lazarus R, Metropolis N, Ulam S. 1956. On certain sequences of integers defined by sieves. Math Mag. 29(3):117–122.
29. Hadamard J. 1896. Sur la distribution des zéros de la fonction zeta(s) et ses conséquences arithmétiques. Bull Soc Math France. 24:199–220.
30. de la Vallée Poussin CJ. 1896. Recherches analytiques la théorie des nombres premiers. Ann Soc Scient Bruxelles. 29:183–256.
31. Selberg A. 1949. An elementary proof of the prime-number theorem. Ann Math. 50:305–313.
32. Erdős P. 1949. Démonstration élémentaire du théorème sur la distribution des nombres premiers. Amsterdam: Mathematisch Centrum.
33. Cramér H. 1936. On the order of magnitude of the difference between consecutive prime numbers. Acta Arith. 2:23.
34. Ingham AE. 1937. On the difference between consecutive primes. Q J Math. 8(1):255–266.
35. Maynard J. 2015. Small gaps between primes. Ann Math. 181(1):383–413.
36. Maynard J. 2016. Large gaps between primes. Ann Math. 183(3):915–933.
37. Ford K, Green B, Konyagin S, Tao T. 2016. Large gaps between consecutive prime numbers. Ann Math. 183(3):935–974.
38. Ford K, Green B, Konyagin S, Maynard J, Tao T. 2018. Long gaps between primes. J Amer Math Soc. 31(1):65–105
39. Grimm R, Weidemüller M, Ovchinnikov YB. 2000. Optical dipole traps for neutral atoms. Adv Atom Mol Opt Phys. 42:95–170.
40. Harte T, Bruce GD, Keeling J, Cassettari D. 2014. Conjugate gradient minimisation approach to generating holographic traps for ultracold atoms. Opt Exp. 22:26548–26558.
41. Bowman D, *et al.* 2017. High-fidelity phase and amplitude control of phase-only computer generated holograms using conjugate gradient minimisation. Opt Exp. 25:11692–11700.
42. Pasienski M, DeMarco B. 2008. A high-accuracy algorithm for designing arbitrary holographic atom traps. Opt Exp. 16:2176–2190.
43. Trypogeorgos D, *et al.* 2013. Precise shaping of laser light by an acousto-optic deflector. Opt Exp. 21:24837–24846.
44. Ryu C, Samson EC, Boshier MG. 2020. Quantum interference of currents in an atomtronic SQUID. Nature Comm. 11:1–6.
45. Tajik M, *et al.* 2019. Designing arbitrary one-dimensional potentials on an atom chip. Opt. Exp. 27:33474–33487.
46. Landau LD, Lifshitz EM. 1977. Quantum mechanics: non-relativistic theory. Oxford: Pergamon Press.
47. Jost R, Kohn W. 1952. Equivalent potentials. Phys Rev. 88:382.
48. Cassettari D, Mussardo G, Trombettoni A. 2022. Data underpinning - Holographic Realization of the Prime Number Quantum Potential, University of St Andrews Research Portal. https://doi.org/10.17630/149e8747-5491-44e0-b897-ae9e7efc15b7.
49. Leanhardt AE, *et al.* 2003. Cooling Bose–Einstein condensates below 500 Picokelvin. Science. 301:1513.
50. Medley P, *et al.* 2011. Spin gradient demagnetization cooling of ultracold atoms. Phys Rev Lett. 106:195301.
51. Haller E, *et al.* 2015. Single-atom imaging of fermions in a quantum-gas microscope. Nat Phys. 11:738–742.
52. Zupancic Ph, *et al.* 2016. Ultra-precise holographic beam shaping for microscopic quantum control. Opt Exp. 24:13881–13893.
53. Posamentier AS, Lehmann I. 2007. The fabulous Fibonacci numbers. New York (NY): Prometheus Book.
54. Gleisberg F, Schleich WP. 2022. Factorization with a logarithmic energy spectrum of a central potential. arXiv:2202.08092. https://doi.org/10.48550/arXiv.2202.08092, preprint: not peer reviewed.
55. Chin C, Grimm R, Julienne P, Tiesinga E. 2010. Feshbach resonances in ultracold gases. Rev Mod Phys. 82:1225.